The Canadian Mineralogist
Vol. 42, pp. 1583-1599 (2004)

SILICATE MELT INCLUSIONS IN PORPHYRY COPPER DEPOSITS: IDENTIFICATION AND HOMOGENIZATION BEHAVIOR

JAMES J. STUDENT AND ROBERT J. BODNAR§

Department of Geosciences, Virginia Tech, Blacksburg, Virginia 24061, U.S.A.

ABSTRACT

Silicate melt inclusions are ubiquitous in phenocrysts in porphyry copper deposits. Compared to melt inclusions in other igneous environments, those in porphyry copper deposits are more difficult to recognize and analyze, for a variety of reasons. The inclusions are usually partially to completely crystallized or altered by hydrothermal fluids, resulting in a dark, granular appearance. In this study, a protocol for identifying and homogenizing crystallized melt-inclusions from porphyry copper deposits is described. The protocol has been used to obtain preliminary data from melt inclusions in the Red Mountain, Arizona, and the Tyrone, New Mexico, porphyry copper deposits. Many melt inclusions in syn- and post-mineralization samples show evidence of alteration by magmatic-hydrothermal fluids that produced alteration and mineralization in the plutons, and many inclusions trapped crystals or fluid (or both) along with the melt. Elevated concentrations of metal in pre-mineralization (H_2O-undersaturated) melt inclusions, and lower concentrations of metal in later syn- and post-mineralization (H_2O-saturated) melt inclusions are consistent with models that invoke quantitative transfer of copper and other metals from the melt into the magmatic aqueous phase when the melt reaches H_2O saturation. Results from Red Mountain and Tyrone are compared to melt inclusions from the White Island, New Zealand, active volcano.

Keywords: melt inclusions, porphyry copper deposits, Red Mountain, Arizona, Tyrone, New Mexico, White Island, New Zealand.

SOMMAIRE

Des reliquats de magma piégés sont répandus dans les phénocristaux des gisements porphyriques cuprifères. En comparaison des reliquats magmatiques d'autres milieux ignés, ceux des gisements porphyriques cuprifères sont plus difficiles à reconnaitre et à analyser, et ce, pour plusieurs raisons. Les inclusions sont généralement cristallisées, en partie ou complètement, ou altérées par des fluides hydrothermaux, avec comme résultat une apparence sombre et granuleuse. Dans ce travail, nous décrivons un protocole pour identifier et pour homogénéiser les reliquats magmatiques cristallisés provenant de gisements porphyriques cuprifères. Ce protocole a été utilisé pour obtenir des données préliminaires portant sur les reliquats magmatiques aux gisements cuprifères de Red Mountain, en Arizona, et de Tyrone, Nouveau-Mexique. Plusieurs reliquats inclus dans des échantillons contemporains ou tardifs par rapport à la minéralisation témoignent d'une altération par des fluides magmatiques et hydrothermaux qui ont produit l'altération et la minéralisation de ces plutons, et plusieurs des inclusions ont piégé cristaux ou fluide (ou les deux) en plus du liquide silicaté. Des teneurs élevées en métaux dans les inclusions de liquide silicaté pré-minéralisation (sous-saturées en H_2O), et des concentrations plus faibles en métaux dans les venues plus tardives par rapport à la minéralisation (saturées en H_2O) concordent avec les modèles faisant appel au transfert quantitatif de cuivre et autres métaux du magma à la phase aqueuse orthomagmatique aussitôt que la saturation en H_2O est atteinte. Les résultats sur les inclusions de Red Mountain et de Tyrone sont comparés aux données sur les reliquats magmatiques provenant de l'île White, en Nouvelle-Zélande, volcan actif.

(Traduit par la Rédaction)

Mots-clés: reliquats magmatiques inclus, gisements porphyriques cuprifères, Red Mountain, Arizona, Tyrone, New Mexico, île White, Nouvelle-Zélande.

§ *E-mail address*: rjb@vt.edu

Introduction

Porphyry copper deposits represent an important economic source of copper and other metals, including molybdenum, gold, silver, zinc and lead (Cox 1986, Guilbert & Parks 1986). Copper and other ore metals are considered to have been extracted from the silicate melt when magmatic fluids exsolved from the magma during crystallization and decompression processes (Burnham 1967, 1979, 1997, Hedenquist & Lowenstern 1994). The metals are later precipitated in an ore shell within and around the pluton as the magmatic fluids cool and mix with externally derived fluids (Beane & Titley 1981).

In this study, we have examined crystallized melt inclusions in quartz phenocrysts from the Red Mountain, Arizona, and Tyrone, New Mexico, porphyry copper deposits in an attempt to develop a protocol for identifying and studying melt inclusions in this ore-forming environment. The inclusions represent magma that was trapped during (Red Mountain) and following (Tyrone) mineralization. In addition, melt inclusions in pre-mineralization Meadow Valley andesite from Red Mountain, Arizona, have been examined in an effort to characterize the early stages of the magmatic system, before the magma evolved to the ore-forming stage. Finally, we have examined melt inclusions in recent lavas of basaltic andesite composition from the active volcanic system at White Island, New Zealand, as a modern analogue representing the very earliest stages in the formation of a porphyry-copper-forming system.

Background Information

Numerous studies over several decades have characterized the physical and chemical environment associated with hydrothermal activity, mineralization, and alteration in porphyry copper deposits (*cf.* Lowell & Guilbert 1970, Beane & Titley 1981, Beane & Bodnar 1995, Roedder & Bodnar 1997). Less information is available concerning the early (pre-mineralization) magmatic stage because the host rocks have generally been altered by later hydrothermal fluids, effectively destroying the original igneous phases and altering the bulk-rock compositions. In addition, in many porphyry copper deposits, the pre- or syn-mineralization volcanic cover has been removed by erosion, thus destroying any information that these rocks might have provided.

Melt inclusions represent samples of melt trapped during crystallization of magmas, and have been used successfully to study magmatic evolution in igneous systems (Clocchiatti 1975, Lowenstern 1995, Roedder 1979, Sobolev 1996, Danyushevsky *et al.* 2002). In volcanic systems in which the rocks cooled rapidly, melt inclusions are commonly preserved as a homogeneous glass (with or without shrinkage bubbles or bubbles containing exsolved volatiles), and are relatively easily recognized and analyzed. Melt inclusions from deeper plutonic environments, or volcanic systems that cooled more slowly, are not only more difficult to recognize, but also present significant analytical challenges (*cf.* Thomas 1994a, b, Yang & Bodnar 1994, Lowenstern 1994, Davidson & Kamenetsky 2001, Frezzotti 2001, Thomas *et al.* 2002, Fedele *et al.* 2003, Rapien *et al.* 2003). In these systems, melt inclusions are preserved as partially devitrified glass or completely crystallized mineral inclusions, usually with a deformed and commonly obscure vapor phase. Such melt inclusions are characteristic of igneous rocks that cooled slowly (Roedder 1979, Lowenstern 1995). The inclusions are commonly dark to opaque in transmitted light (owing to the presence of abundant crystallites) and are not easily recognized during routine petrographic examination (see Fig 1, inclusions at 22°C).

For most inclusions that contain only glass (± a vapor bubble), one need only to expose the inclusion at the surface before conducting analyses. However, to study crystallized melt inclusions, it is necessary to first homogenize the inclusion to a glass. Halter *et al.* (2002) described a technique for analyzing crystallized melt inclusions without the need for re-homogenization, using laser-ablation ICP–MS. Whereas this technique is indeed applicable for determining concentrations of many elements of interest in melt inclusions, other important chemical and petrological information may be lost. For example, observation of melt inclusions during heating provides information concerning the order and temperature at which various phases dissolve, which in turn can be used to infer the trapping environment of the melt inclusion (*i.e.*, on the H_2O-saturated solidus or on a cotectic; Student & Bodnar 1999); such observations can help to identify solids that have been trapped along with the melt (*cf.* Fedele *et al.* 2003). In addition, information concerning the volatile (H_2O, CO_2) budget of the melt is not available from LA–ICP–MS analyses, and this information is critical to understanding ore-forming processes in magmatic hydrothermal systems. The protocol described here allows one to: (1) determine the temperature of trapping of the melt, (2) identify those inclusions that have trapped only a single, homogeneous melt phase (based on the order and consistency of phase changes within a group of coeval melt inclusions during heating), and (3) produce a homogeneous glass phase that may be analyzed for major, minor and trace elements, including volatile components.

Sample Description

Rock samples

Samples of quartz latite from Red Mountain, Arizona, were obtained from a depth of approximately 1,500 m in drill hole 148 (Corn 1975). Unaltered Meadow Valley andesite was collected from the surface

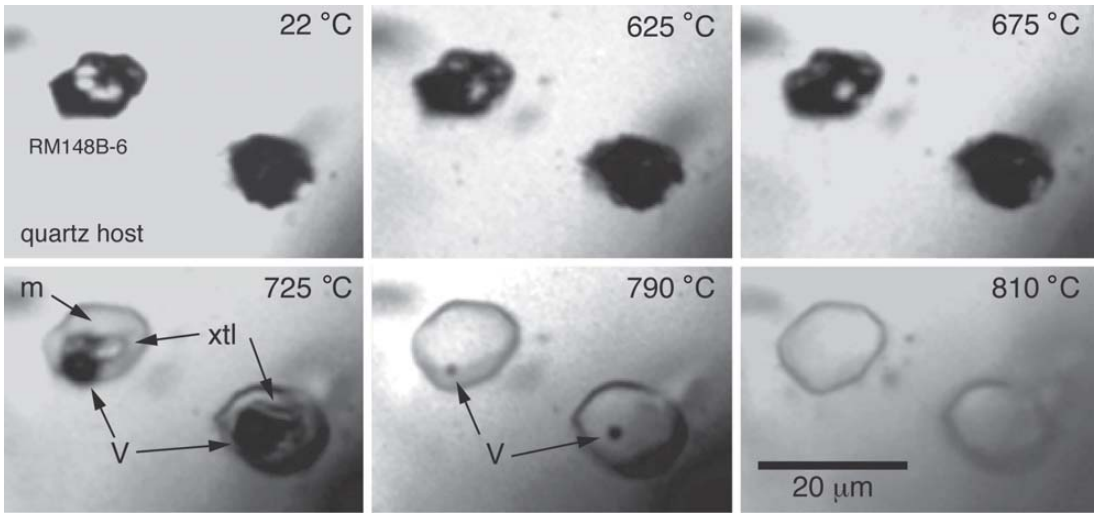

FIG. 1. The change in appearance of two crystallized silicate-melt inclusions in a quartz phenocryst from a quartz latite dike at Red Mountain, Arizona, during heating from room temperature (22°C) to the homogenization temperature (810°C). Evidence for melting is first observed at 675°C. By 725°C, the volatiles (V) have coalesced into a single, spherical bubble in the melt, and feldspar daughter minerals (xtl) are noticeably reduced in size. At 790°C, each inclusion contains a small feldspar crystal (not visible) in contact with the vapor bubble. The vapor bubble and feldspar are still present after heating to 800°C, but are gone after heating to 810°C. Simultaneous disappearance of vapor and crystal indicates that the melt was trapped on the H_2O-saturated quartz–feldspar cotectic. These inclusions were heated under 1 kbar confining pressure in a TZM vessel. The inclusion labeled RM148B–6 was analyzed by EPMA, and its composition is listed in Table 1.

on the northeastern side of Red Mountain. This same andesite was encountered in drill core, but the phenocrysts (plagioclase and pyroxene) had been destroyed by alteration, and could not be used for melt-inclusion studies.

Surface samples of monzonite and quartz monzonite were collected from the pit and surrounding country-rock at the Tyrone porphyry copper deposit, New Mexico. Samples represent the four main periods of magmatism (Duhamel *et al.* 1995), but only the unfractured and unmineralized quartz monzonite of Stage IV contains relatively isolated melt inclusions suitable for study. This rock is a post-mineralization member of the overall magmatic system that produced the Tyrone deposit. We assume that it represents a sample of a productive magma after it has lost its metals to the magmatic-hydrothermal fluid.

Results from the porphyry copper deposits at Red Mountain and Tyrone were compared to melt inclusions from White Island, New Zealand, which represents a young porphyry-copper-forming system that has not yet reached the productive stage (Rapien 1998, Rapien *et al.* 2003). The White Island basaltic andesite is interpreted to be analogous to early, pre-mineralization volcanic rocks in porphyry copper systems, such as the Meadow Valley andesite at Red Mountain.

Additional details concerning sample selection and analytical techniques are available in Student (2002).

Melt inclusions

Melt inclusions examined in this study show variable proportions of glass, crystals and vapor. Some melt inclusions in pyroxene from the Meadow Valley andesite at Red Mountain and all inclusions in pyroxene and plagioclase from White Island contain only glass + vapor. Other inclusions (in pyroxene) from the Meadow Valley andesite contain one or more crystals in addition to vapor and glass. Plagioclase daughter crystals (identified on the basis of polysynthetic twinning and electron-microprobe data) have been identified in some of these inclusions. All inclusions in quartz from the Red Mountain quartz latite and from Tyrone are completely crystallized and contain distorted vapor bubbles that fill the interstices between the daughter crystals and the host walls. The largest daughter mineral occupies >50% of the inclusion volume and has been identified as feldspar ($An_{11–40}$) based on electron-microprobe analysis (EPMA) and optical characteristics. The variable phase relations observed in melt inclusions reflect the different rates of cooling of the melt inclusions (and host rocks) following entrapment, with glass-bearing inclu-

sions generally assumed to have cooled more rapidly than crystallized or crystal + glass inclusions of the same size (Roedder 1979, 1984). In addition, many of the melt inclusions trapped mixtures of melt ± crystals ± fluid, as indicated by results of heating experiments described below.

The melt inclusions studied in some cases occur along growth zones or along trails, but the majority of inclusions observed in quartz phenocrysts from Red Mountain occur as isolated individual inclusions, or small groups of inclusions, within phenocrysts. At White Island, coexisting melt and solid inclusions (plagioclase inclusions in pyroxene and pyroxene inclusions in plagioclase) commonly occur along the same growth zone (Rapien 1998). The size of the melt inclusions ranges from about 20 to 50 μm in the Red Mountain andesite, from <5 to about 25 μm in the Red Mountain quartz latite, and from <5 to about 35 μm in the Tyrone quartz monzonite. At White Island, the inclusions are generally less than 20 μm in diameter. Larger inclusions occur in all samples from all of the locations studied, but these generally show evidence of natural decrepitation, such as a halo of smaller inclusions surrounding a larger central inclusion, or radial fractures extending from the inclusion (Vityk & Bodnar 1995, Vityk *et al.* 1995, Bodnar 2003); also, they may be intersected by planes of secondary aqueous inclusions that altered the inclusion contents, or such inclusions decrepitated during heating to homogenize the contents.

Analytical Techniques

Sample preparation

Doubly polished thin sections 30 μm and 1.5 mm thick were prepared from all samples, with the thickness varying as a function of phenocryst size and clarity. Sections were examined petrographically, and those samples containing recognizable melt inclusions were selected for further study. Note that the term "recognizable" is somewhat misleading in that most crystallized melt inclusions would not be recognizable as such by many petrographers who are unfamiliar with this subject. Most of the inclusions appear as dark, irregular areas within the host, occasionally with discernible crystals and bubbles (Fig. 1; inclusions at 22°C). It is only after the inclusions are heated to produce a homogeneous glass (± vapor bubble) that one can be reasonably certain that the feature was indeed a crystallized melt-inclusion.

Phenocrysts (quartz, plagioclase, and pyroxene) with melt inclusions were removed from the thin section by scoring the sample and glass slide using a diamond scribe, and then removing the portion of the sample containing the phenocryst. The size of the area removed ranged from about 1 mm to 1 cm in maximum dimension. Quartz phenocrysts ranging in size from about 1 mm to 1 cm were also obtained by crushing the rock in a mini jaw crusher, followed by hand picking under a binocular microscope. Pyroxene phenocrysts were extracted from andesite by crushing followed by sieving and magnetic separation. Phenocrysts removed by crushing were mounted on glass slides and ground to produce a flat surface and then polished. The phenocrysts were then removed from the slide and remounted with the polished side down, and the second side was ground and polished to produce doubly polished wafers. In some cases, quartz phenocrysts were mounted with the *c* axis either parallel or perpendicular to the glass slide to facilitate identification of growth zones containing primary fluid inclusions.

During heating to homogenize crystallized melt-inclusions, groundmass adhering to phenocrysts usually begins to melt before the melt inclusions are completely homogenized, degrading the optical quality and, in some cases, causing the host phase to melt. Groundmass melting also caused the sample to adhere to the heating stage or the platinum capsule after quenching. To minimize these problems, groundmass attached to phenocrysts was removed by gently abrading away the material with a diamond scribe, as described by Student (2002). For some samples, the surrounding matrix could not be removed mechanically. In this case, the sample (quartz phenocryst) was placed in concentrated hydrofluoric acid (HF diluted with 50% H_2O) for several seconds to two minutes, similar to the technique described by Anderson (1991). Acid cleaning also highlighted fractures connecting melt inclusions with the outer surface; such inclusions likely lost (or gained) volatiles and perhaps other components after trapping and were avoided during analysis. However, as described below, even with these precautions, several of the inclusions analyzed had apparently re-equilibrated with external hydrothermal fluids following trapping.

After homogenizing the inclusions (as described below), host phenocrysts were ground and polished by hand to expose homogenized melt inclusions for electron-microprobe analysis. Phenocrysts were mounted with Superglue on a round glass slide 2.5 cm in diameter. Care was taken to insure that the adhesive lapped up the sides of the phenocryst to prevent plucking and scratching during polishing. Grinding and polishing were accomplished with 5, 3, 1, and 0.25 μm diamond pastes on cloth mounted on glass plates. A polishing jig described by Naney (1984) was used to control the amount of sample being ground away and to prevent wedging of the sample. The slide was attached to the polishing device with double-sided tape so that the sample could be easily removed to monitor progress using reflected light microscopy.

Techniques for homogenization of melt inclusions

As noted above, the major difficulty in working with melt inclusions from porphyry copper deposits (and other deep plutonic environments) is that the inclusions

have crystallized following entrapment. Thus, our first goal was to develop a technique to homogenize the inclusions without loss of any of the inclusion's contents. Other investigators have homogenized partially or completely crystallized melt-inclusions (*cf.* Skirius *et al.* 1990), but the inclusions generally contained less H_2O (and other volatiles) than the inclusions described here, and the host phases were not crosscut by the abundant trails of aqueous fluid inclusions common in quartz phenocrysts from porphyry copper deposits. Thus, the two factors that complicated homogenization of melt inclusions in this study were: (1) decrepitation of volatile-rich melt inclusions during heating, and (2) the abundance of primary and secondary aqueous fluid inclusions that decrepitated during heating, fracturing the host phase and opening the melt inclusions (Webster *et al.* 1997). Three methods were evaluated in the course of this study to homogenize melt inclusions: 1) heating in a microscope heating stage, 2) heating in a 1-atmosphere vertical tube furnace, and 3) heating under pressure in a cold-seal pressure vessel.

Crystal-bearing melt inclusions in quartz phenocrysts were initially heated on a programmable Linkam TS1500 heating stage. Homogenizing melt inclusions under the microscope is the preferred method because the inclusions can be monitored continuously during heating. This allows the homogenization temperature to be determined more precisely (compared to step-heating, described below) and allows one to observe any changes that might occur during cooling (such as nucleation of a vapor or shrinkage bubble or precipitation of daughter minerals). The stage was flushed with an argon + 1% H_2 gas mixture to minimize oxidation during heating. Samples were heated at 30°C/min from room temperature to 500°C. The sample was then heated at a rate of 10°C/min until first melting was observed. At this point, a heating rate of 1–2°C/min was used until homogenization was achieved, as indicated by either the complete dissolution of the last visible crystal or vapor bubble. In some cases, the final crystal and bubble disappeared at the same temperature. A complete run lasted about 3 hr. Some investigators have suggested that long duration heating may lead to loss of water from quartz-hosted inclusions. However, Skirius *et al.* (1990) reported only minimal loss of H_2O (several tenths of a percent) from inclusions in quartz that were heated to 800°–900°C for 20 hr.

The majority of heating runs in the Linkam stage failed owing to decrepitation of mostly secondary aqueous fluid inclusions located near melt inclusions. Such behavior was also reported by Webster *et al.* (1997). In addition, nearly all melt inclusions greater than about 15 μm decrepitated before homogenization, presumably because of high internal pressures generated during heating of melt inclusions with high H_2O contents (Student & Bodnar 1996). Only two successful determinations of homogenization temperature were obtained with the Linkam stage, and both of these were higher (by about 100°C; Table 1) than those obtained by heating the sample under pressure, as discussed below. In an attempt to eliminate the decrepitation problem, several phenocrysts were heated in a 1 atm vertical tube furnace following the procedure described by Webster *et al.* (1997) and Student & Bodnar (1999). After heating, polished sections were prepared from the phenocrysts. We anticipated that by heating the entire phenocryst before grinding and polishing, the additional surrounding host-material might prevent or minimize decrepitation of melt-inclusions. However, as with inclusions heated in the Linkam stage, decrepitation of the abundant secondary aqueous fluid inclusions fractured the host phenocryst in the vicinity of melt inclusions, causing most melt-inclusions to leak.

The method that proved most successful to homogenize crystallized melt inclusions involved heating samples in a TZM (Titanium – Zirconium – Molybdenum alloy) cold-seal pressure vessel. The phenocrysts were placed in a 5 mm long, 5 mm OD platinum capsule and loaded into the pressure vessel. The capsule was pierced with a needle before being placed into the pressure vessel to permit the argon pressure medium to freely enter the capsule at run conditions to prevent collapse of the capsule and possible crushing of the sample. The vessel was sealed and pressurized with argon to 300–500 bars, then lowered into a preheated furnace. As the TZM vessel was heated, pressure increased. When the pressure reached about 1000 bars, argon was bled off during continued heating, to maintain the pressure at about 1000 bars, and the pressure was fixed at 1000 bars after the temperature stabilized.

The protocol for homogenizing the melt inclusions in a pressure vessel consists of two stages. During stage one, the goal is to determine the lowest temperature that will result in homogenization of a significant proportion of the inclusions. We contend that those inclusions with the lowest temperature of homogenization are most likely to have trapped a single, homogeneous phase and to have not re-equilibrated following trapping, because trapping multiple phases or the loss of H_2O or other components following entrapment both result in an increase in the temperature of homogenization. To determine the minimum temperature of homogenization, one or a few phenocrysts from one sample were heated incrementally. Once the minimum temperature was determined in this way, several phenocrysts from the same sample were heated to that temperature in one step and held there for 24 hours.

In stage one, the sample was initially heated to 550°C (in about 20 minutes) and held at this temperature for 24 hours. The vessel was then removed from the furnace and quenched in water at a rate in excess of 600°C per second. After quenching, the sample was removed from the TZM vessel and observed with a microscope (Fig. 1). If the inclusion had not completely homogenized (*i.e.*, the inclusions in Fig. 1 at 625°, 675°, 725° and 790°C), the sample was reinserted into the vessel as

Table 1. Homogenization temperatures and compositions of melt inclusions.

Sample	Th °C	SiO_2	TiO_2	Al_2O_3	FeO	MnO	MgO	CaO	Na_2O	K_2O	P_2O_5	Ba	Cl	Total	Zn	Cu	H_2O^*
Red Mountain quartz latite melt inclusions																	
RM148B-1	915	75.19	0.05	12.43	0.53	0.06	0.04	0.69	1.32	2.12	0.02		0.09	92.55	7	11	7.5
RM148B-2	915	74.15	0.08	12.90	0.28	0.03	0.07	0.55	1.56	1.85	0.03		0.14	92.64	7	10	7.4
RM148B-3	825	76.86	0.07	13.24	0.42	0.02	0.07	0.68	2.80	2.69	0.05	0.03	0.13	96.68	8	10	3.3
RM148B-4	825	76.10	0.11	10.90	0.22	0.01	0.04	0.54	5.66	2.21	0.04	0.03	0.09	95.95	9	13	4.1
RM148A-1	810	74.97	0.09	12.08	0.38	0.03	0.05	0.59	1.45	2.36	0.06	0.05	0.12	92.23	9	13	7.8
RM148B-5	835	74.67	0.12	12.80	0.42	0.02	0.08	0.66	5.40	2.41			0.12	96.70	7	11	3.3
RM148B- 6 (RMD2)	810	73.95	0.07	13.15	0.41	0.00	0.03	0.67	4.37	2.45			0.13	95.23	8	13	4.8
RM148A-2	810	77.32	0.09	12.01	0.37	0.03	0.04	0.62	0.34	2.45	0.09	0.06	0.14	93.56	7	9	6.4
RM148A-3	810	75.58	0.10	12.38	0.54	0.03	0.11	0.66	0.38	2.61	0.04	0.04	0.15	92.62	9	17	7.4
RM148B-7	835	74.84	0.20	11.38	0.44	0.01	0.05	0.07	5.00	2.45			0.12	94.56	8	15	5.4
RM148B-8*	810	76.37	0.07	10.77	0.41	0.00	0.03	0.67	4.37	2.45			0.13	95.27	8	13	4.7
Average MI		75.36	0.10	12.33	0.40	0.02	0.06	0.63	3.45	2.36	0.05	0.04	0.12	94.92	8	12	5.7
Red Mountain andesite melt inclusions																	
RMMVA-1	1169	55.90	0.99	11.07	7.48	0.20	6.63	11.57	3.23	2.21	0.04	0.08	0.02	99.42	65	336	0.6
RMMVA-2	1165	55.16	0.81	10.29	8.06	0.23	8.82	12.94	2.73	1.44	0.23	0.10	0.03	100.85	81	282	-0.9
RMMVA-3	1172	56.36	1.38	11.27	6.25	0.12	5.17	12.58	3.23	2.95	0.42	0.15	0.12	99.99	76	346	0.0
RMMVA-4	1170	56.22	1.15	11.46	6.25	0.07	5.47	12.40	2.66	3.17	0.20	0.10	0.17	99.30	68	362	0.7
RMMVA-5	1168	53.95	0.89	11.71	7.55	0.22	9.54	11.83	2.04	1.92	0.26	0.00	0.11	100.03	50	356	0.0
RMMVA-6	1168	54.37	1.25	11.00	7.52	0.15	9.56	11.72	1.79	1.81	0.60	0.03	0.06	99.84	55	277	0.2
RMMVA-7	1170	53.52	1.02	11.21	7.39	0.21	9.00	11.45	1.77	1.93	0.32	0.04	0.06	97.93	73	312	2.1
RMMVA-8	1177	54.30	1.14	11.97	6.51	0.17	8.57	12.06	2.80	0.53	0.16	0.05	0.04	98.30	66	346	1.7
RMMVA-9	1175	54.77	1.00	11.96	6.82	0.14	8.37	11.69	2.76	1.95	0.28	0.11	0.16	100.00	60	329	0.0
RMMVA-10	1170	54.43	1.09	11.42	5.83	0.11	8.36	13.29	2.79	1.61	0.29	0.10	0.13	99.43	57	368	0.6
RMMVA-11	1172	55.27	0.90	11.63	6.08	0.11	8.47	12.73	2.72	1.17	0.25	0.08	0.12	99.53	54	329	0.5
Average MI		54.93	1.06	11.36	6.89	0.16	8.00	12.21	2.59	1.88	0.28	0.08	0.09	99.52	64	331	0.5
Red Mountain andesite melt inclusions (unhomogenized)																	
RMMVA-12		67.05	0.61	16.00	0.33	0.04	0.08	0.80	4.02	6.17	0.68	0.11	0.25	96.13	88	457	3.9
RMMVA-13		67.41	0.58	16.88	0.45	0.03	0.08	0.76	3.83	6.18	0.48	0.13	0.25	97.06	80	398	2.9
RMMVA-14		66.81	0.54	16.44	0.42	0.02	0.04	0.81	3.67	6.41	0.57	0.19	0.23	96.14	81	424	3.9
RMMVA-15		67.97	0.54	16.93	0.29	0.01	0.05	0.78	3.98	6.20	0.59	0.17	0.27	97.80	84	458	2.2
RMMVA-16		66.76	0.57	16.83	0.39	0.03	0.08	0.84	4.29	6.15	0.44	0.12	0.19	96.68	77	432	3.3
RMMVA-17		66.16	0.56	18.03	2.02	0.00	0.13	1.21	4.42	5.55	0.30	0.09	0.25	98.71	88	432	1.3
RMMVA-18		66.38	0.42	17.93	0.41	0.06	0.14	1.23	4.59	5.61	0.35	0.12	0.24	97.48	77	377	2.5
RMMVA-19		62.69	0.61	13.37	4.67	0.13	4.54	5.16	3.17	4.52	1.38	0.05	0.19	100.48	84	411	-0.5
RMMVA-20		62.83	0.83	13.12	4.65	0.14	4.38	5.44	3.06	4.39	1.20	0.09	0.10	100.22	79	390	-0.2
RMMVA-21		61.92	0.84	13.11	4.78	0.12	4.49	5.35	3.10	4.43	1.07	0.20	0.14	99.54	83	431	0.5
RMMVA-22		61.91	0.88	13.20	4.62	0.10	3.47	6.02	2.91	4.80	0.39	0.06	0.18	98.55	73	388	1.5
RMMVA-23		63.25	0.98	12.96	4.78	0.03	3.70	4.65	3.62	4.42	0.28	0.09	0.15	98.91	83	439	1.1
RMMVA-24		64.15	0.95	13.62	4.43	0.11	3.70	4.48	3.08	4.65	0.45	0.11	0.17	99.89	78	416	0.1
Average MIUH		65.02	0.69	15.26	2.48	0.06	1.91	2.89	3.67	5.34	0.63	0.12	0.20	98.28	81	419	1.7
Tyrone quartz monzonite melt inclusions																	
Ty-1	805	75.37	0.11	13.23	0.32	0.01	0.06	0.53	3.36	3.27	0.04	0.04	0.09	96.42	4	5	3.6
Ty-2	805	75.05	0.02	13.08	0.35	0.01	0.04	0.54	3.18	3.22	0.09	0.04	0.08	95.71	3	3	4.3
Ty-3	805	74.71	0.06	12.64	0.38	0.01	0.05	0.50	2.46	3.18	0.01	0.03	0.08	94.11	5	5	5.9
Ty-4	820	71.97	0.07	14.72	0.43	0.07	0.07	0.46	2.43	5.92	0.03	0.03	0.14	96.34	4	7	3.7
Ty-5	820	71.38	0.08	15.14	0.44	0.06	0.08	0.47	2.45	6.21	0.03	0.05	0.15	96.54	3	13	3.5
Ty-6	820	74.00	0.22	13.39	0.47	0.07	0.06	0.42	3.11	4.62	0.04	0.04	0.58	97.01	5	7	3.0
Ty-7	805	76.09	0.07	12.55	0.32	0.01	0.05	0.60	3.25	3.39	0.02	0.04	0.11	96.50	5	7	3.5
Ty-8	805	75.51	0.07	11.83	0.27	0.01	0.05	0.59	2.32	3.09	0.06	0.03	0.08	93.90	6	8	6.1
Ty-9	805	75.37	0.08	11.56	0.27	0.02	0.04	0.56	2.01	3.10	0.07	0.06	0.06	93.19	4	5	6.8
Ty-10	820	73.70	0.06	13.57	0.53	0.08	0.07	0.34	2.61	5.63	0.07	0.03	0.12	96.81	4	7	3.2
Ty-11	820	72.43	0.07	14.11	0.56	0.07	0.05	0.36	2.68	5.73	0.03	0.02	0.14	96.25	4	6	3.7
Ty-12	820	72.79	0.07	15.06	0.62	0.08	0.07	0.43	2.65	5.94	0.05	0.09	0.16	98.01	2	3	2.0
Ty-13	820	73.53	0.08	11.73	0.25	0.03	0.03	0.48	3.11	3.30	0.02	0.06	0.10	92.72	3	6	7.3
Ty-14	820	75.84	0.02	11.83	0.28	0.00	0.03	0.62	2.38	3.42	0.00	0.06	0.11	94.59	4	6	5.4
Ty-15	820	74.07	0.02	12.16	0.23	0.01	0.06	0.57	4.73	3.60	0.12	0.04	0.08	95.69	3	2	4.3
Ty-16	820	75.41	0.17	13.05	0.40	0.09	0.07	0.52	3.20	4.32	0.10	0.02	0.41	97.76	3	6	2.2
Ty-17	805	75.96	0.10	13.36	0.53	0.02	0.05	0.51	4.32	3.19	0.05	0.02	0.09	98.20	6	5	1.8
Ty-18	805	71.02	0.04	13.27	0.37	0.03	0.02	0.49	3.38	3.32	0.14	0.03	0.06	92.17	5	5	7.8
Ty-19	805	71.56	0.05	10.65	0.56	0.06	0.10	0.16	5.86	3.16	0.02	0.04	0.15	92.37	4	6	7.6
Ty-20	805	73.25	0.09	11.14	0.31	0.01	0.05	0.42	2.99	2.87	0.01	0.03	0.05	91.22	5	8	8.8
Ty-21	820	75.72	0.08	12.60	0.36	0.03	0.07	0.58	4.55	3.36	0.11	0.03	0.08	97.57	4	5	2.4
Average MI		74.04	0.08	12.89	0.39	0.04	0.06	0.48	3.19	3.99	0.05	0.04	0.14	95.39	4.	6	4.6
White Island andesite melt inclusions																	
WI-1		62.00	0.86	16.78	4.84	0.08	1.81	6.18	3.50	2.11				98.16	75	383	1.8
WI-2		59.95	0.88	16.99	4.91	0.12	1.86	6.87	3.65	1.90				97.13	67	357	2.9
WI-3		58.95	0.90	18.77	4.58	0.08	1.46	7.56	3.10	1.81				97.21	60	343	2.8
WI-4		65.98	0.92	15.55	5.62	0.08	2.01	5.16	4.20	2.23				101.75	73	379	-1.8
WI-5		61.30	0.59	18.12	3.57	0.03	1.58	7.67	3.95	1.61				98.42	65	348	1.6
WI-6		64.21	1.12	14.51	7.35	0.11	2.04	5.79	1.93	2.27				99.33	58	330	0.7
Average MI		62.07	0.88	16.79	5.15	0.08	1.79	6.54	3.39	1.99				98.67	66	357	1.3

described above, and heated to a higher temperature for an additional 24 hours. The sample was then quenched, removed from the vessel, and re-examined. The heating steps ranged from 50°C to 5°C, with smaller steps used as the homogenization temperature was approached. This procedure was repeated until total homogenization occurred (*i.e.*, the inclusions in Fig. 1 after heating to 810°C). In most samples, a large portion of the melt inclusions homogenized over a range of a few tens of degrees; at this point, the heating experiment was stopped. If heating were continued in an attempt to homogenize all inclusions in the phenocryst, those that homogenize at lower temperatures would have decrepitated or changed composition by dissolving excess silica from the quartz host. Moreover, those inclusions that did not homogenize commonly contained either large vapor bubbles or large crystals, or both, indicating that those inclusions had trapped an aqueous phase, or a solid phase, or both, along with the melt. Once the homogenization temperature for a particular sample had been determined by this step-heating procedure, using only one or a few phenocrysts from the sample, other phenocrysts from the same sample were heated to that temperature in a single step to minimize the loss of volatiles or other possible re-equilibration associated with heating melt inclusions (Qin *et al.* 1992, Nielsen *et al.* 1998, Danyushevsky *et al.* 2000). The sample was held at temperature for 24 hours, on the basis of results of a study of synthetic silicate melt inclusions. This amount of time gave the most reliable (accurate) temperature of homogenization (Student & Bodnar 1999).

Decrepitation of melt inclusions during heating to homogenization encountered with the Linkam and 1 atm furnace techniques was significantly reduced by heating the inclusions under pressure. However, even under these conditions, the larger inclusions (greater than about 30–50 μm) still decrepitated. Other investigators (Sterner & Bodnar 1989, Skirius *et al.* 1990, Schmidt *et al.* 1998) have previously shown that heating aqueous or melt inclusions under a confining pressure eliminates (or minimizes) decrepitation.

Melt inclusions in pyroxene and plagioclase phenocrysts from the Meadow Valley andesite were homogenized using a Vernadsky stage (Sobolev *et al.* 1980). These inclusions could be homogenized at one atmosphere without decrepitation owing to the lower H_2O contents of these melts and the absence of planes of secondary aqueous inclusions.

Electron-Microprobe Analysis (EPMA)

Quantitative analyses were performed at Virginia Tech on a Cameca SX50 electron microprobe, equipped with four wavelength-dispersion spectrometers. For SiO_2, TiO_2, Al_2O_3, FeO, MnO, MgO, CaO, Na_2O, K_2O, BaO, P_2O_5 and Cl, analysis and standardization were performed using silicate, oxide, phosphate and glass standards, and the data were corrected with the PAP method developed by Pouchou & Pichoir (1985) using vendor-supplied software. Copper and zinc concentrations were also determined for several melt inclusions by EPMA. These analyses were complicated by the fact that the majority of the inclusions that could be homogenized successfully are small (<15 μm), and Cu and Zn are present in the inclusions at or near the detection limits. The analytical conditions for measuring trace concentrations of Cu and Zn recommended by Fialin *et al.* (1999), Lynton *et al.* (1993) and Williams *et al.* (1995) were used here. Analyses of standards and inclusions for Cu and Zn were performed at 35 kV, using a current of 50 nA with a 10 μm rastered beam. During the analysis, a pit was burned into the NIST standard glasses and inclusion glasses owing to the high beam-current. For this reason, melt inclusions were analyzed for the major and minor elements before being analyzed for Cu and Zn.

RESULTS

Homogenization temperatures

Homogenization temperatures were determined either by monitoring melt inclusions during continuous heating under the microscope using the Linkam or Vernadsky stages, or by examining inclusions following each heating step in the one-atmosphere furnace or the TZM pressure vessel. We emphasize that the primary goal of heating melt inclusions was not to determine the homogenization temperature, but rather to obtain a homogeneous glass for EPMA analysis. Having said this, the observed temperatures of homogenization and the consistency of these temperatures within a given sample, combined with the good agreement between the measured temperatures and those predicted by thermodynamic models as described below, suggest that temperatures of homogenization determined in the pressure-vessel experiments closely approximate the actual trapping temperatures. Temperatures of homogenization of melt inclusions in pyroxene and plagioclase from the Meadow Valley Andesite at Red Mountain, Arizona, range from 1165° to 1177°C (Table 1, Fig. 2). Seven melt inclusions in plagioclase homogenized (in the Vernadsky stage) by disappearance of the vapor bubble at 1175°C, but during quenching the melt recrystallized and the phenocryst shattered. These inclusions were not analyzed and are not included in Table 1. During heating, phases in melt inclusions in pyroxene homogenized in the order plagioclase (1070°–1120°C), opaque phases (1135°–1165°C), vapor bubble (1155°–1177°C). The inclusion size increased noticeably during heating as pyroxene melted from the walls. The consistency in the order in which phases homogenized, and the narrow range in temperature over which this occurred, suggest that all of the inclusions have similar compositions and trapped only melt, and this interpretation is supported by EPMA analyses of the melt inclusions (Table 1, Fig. 3).

Melt inclusions in quartz from the Red Mountain quartz latite homogenized in the range 810° to 915°C (Table 1, Fig. 2). The two inclusions that homogenized at 915°C were heated using the Linkam stage. Eight other inclusions heated in the TZM vessel homogenized between 810° and 835°C. For reasons described later, we believe that temperatures of homogenization of inclusions heated under elevated confining pressure in the TZM vessel more closely represent the actual temperatures of formation. Recognizable melting of the inclusions began at about 675°C, and final homogenization occurred either by dissolution of the vapor bubble into the melt (Fig. 1), or by the simultaneous disappearance of plagioclase and the vapor bubble. Note that only about 1/3 to 1/2 of the melt inclusions in the samples showed the expected behavior. Most of the larger inclusions decrepitated during heating, and many inclusions still contained large crystals, or large vapor bubbles, or both, after heating was stopped. These are interpreted to represent inclusions that trapped a solid or aqueous phase, or both, along with the melt, or that re-equilibrated either following entrapment in nature or during heating in the laboratory. This observation emphasizes the need to homogenize crystallized melt-inclusions before conducting chemical analyses in order to distinguish between those inclusions that trapped only melt (and did not re-equilibrate after trapping) and those that trapped multiple phases or re-equilibrated after trapping. As with melt inclusions in pyroxene described above, a significant amount of quartz was dissolved from the inclusion walls during heating, and many inclusions showed a negative crystal shape after homogenization (Fig. 1).

Quartz-hosted melt inclusions from Stage IV at Tyrone homogenized between 805° and 835°C (Table 1, Fig. 2). As with the quartz-hosted inclusions from Red Mountain, successful homogenization was indicated by the simultaneous disappearance of plagioclase and vapor bubble, or by dissolution of the vapor bubble into the melt after dissolution of the last daughter mineral. Many inclusions failed to homogenize, and these are interpreted to represent inclusions that trapped melt ± crystals ± fluid.

Melt inclusions from White Island contain only glass (± bubble), and were not heated before analysis.

Melt composition

Major-element compositions of melt inclusions and host phenocrysts from Red Mountain, Arizona, and Tyrone, New Mexico, are plotted on Harker variation diagrams in Figure 3. The data are also listed in Table 1, along with data for TiO_2, MnO, P_2O_5, Ba, Cl, Cu and Zn. Whereas the compositions show significant variabil-

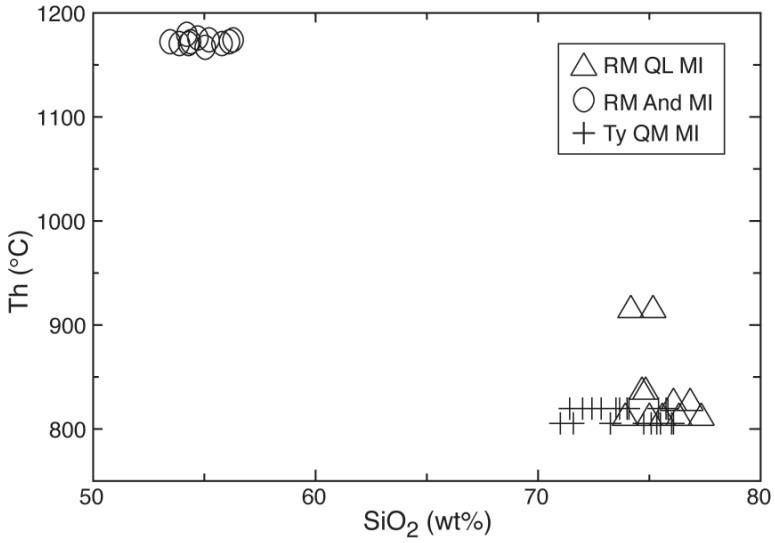

FIG. 2. Temperature of homogenization *versus* SiO_2 content for melt inclusions in Red Mountain, Arizona, andesite and quartz latite and in Tyrone, New Mexico, quartz monzonite. The Red Mountain quartz latite melt inclusions with temperatures of homogenization above 900°C were measured in the Linkam microscope heating stage. All other Red Mountain quartz-latite-hosted melt inclusions and the Tyrone quartz-monzonite-hosted melt inclusions were homogenized in a TZM pressure vessel at 1 kbar confining pressure. Melt inclusions in the Red Mountain andesite were homogenized in the Vernadsky stage (Sobolev *et al.* 1980).

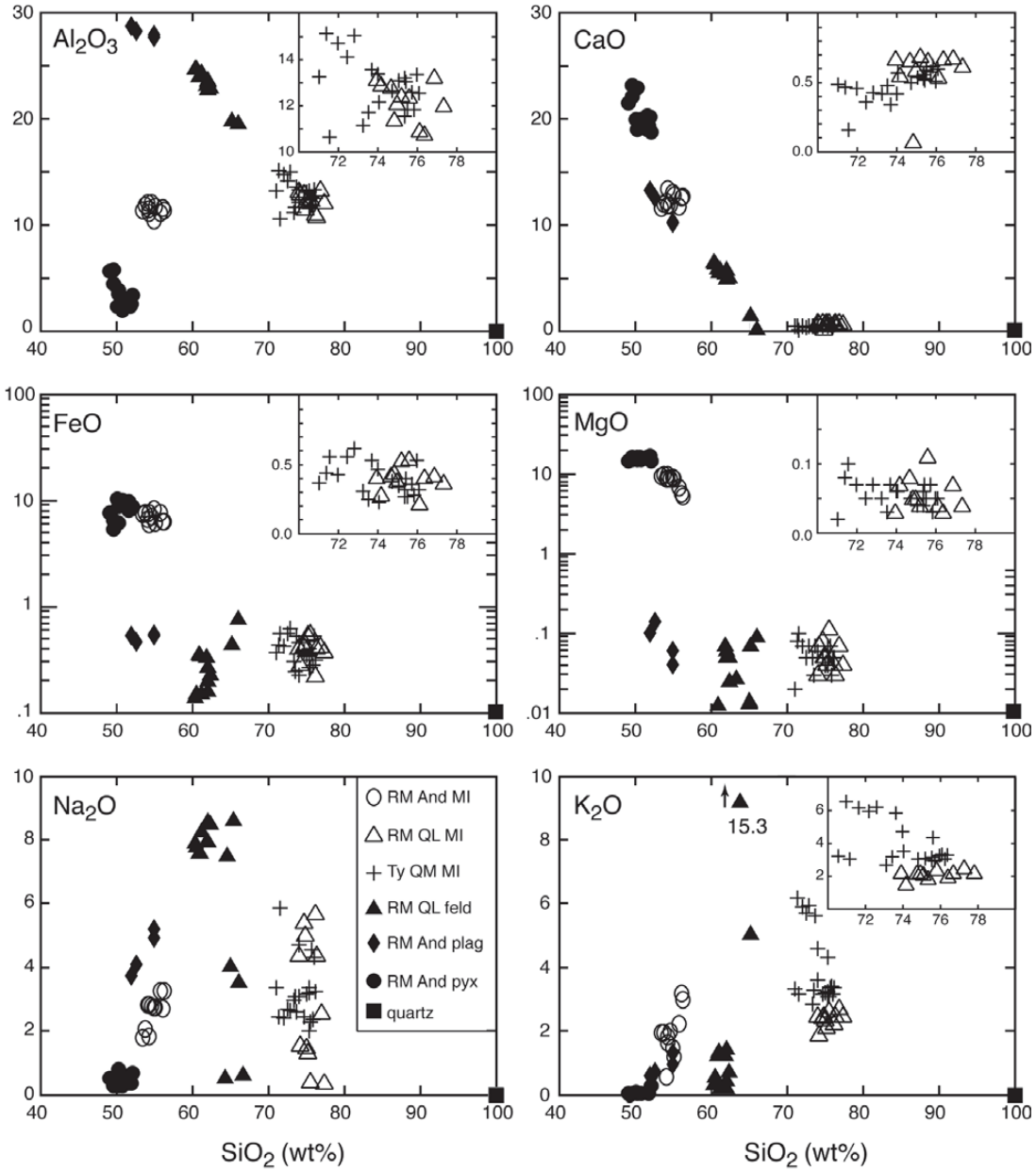

FIG. 3. Harker variation diagrams showing concentrations of Al_2O_3, FeO, MgO, CaO, Na_2O, and K_2O as a function of SiO_2 concentration. Note that the ordinates for the FeO and MgO plots are logarithmic, but the inset diagrams are all plotted on a linear scale. The open oval symbol (*RM And MI*) represents melt inclusions in pyroxene phenocrysts from Red Mountain, Arizona, andesite. The open triangle symbol (*RM QL MI*) represents melt inclusions in quartz phenocrysts from Red Mountain, Arizona, quartz latites. The cross symbol (*Ty QL MI*) represents melt inclusions in quartz phenocrysts from Tyrone, New Mexico, quartz monzonite. The filled triangle symbol (*RM QL feld*) represents feldspar inclusions in quartz phenocrysts from Red Mountain, Arizona, quartz latites. The filled diamond symbol (*RM And plag*) represents groundmass plagioclase in andesite from Red Mountain, Arizona. The filled oval symbol (*RM And pyx*) represents pyroxene phenocrysts in andesite from Red Mountain, Arizona. The filled square symbol (*quartz*) represents the composition of quartz. Compositions of host phases (quartz, plagioclase, pyroxene) are plotted to facilitate identification of those compositions that may be contaminated by the host phase (either by incorrect placement of the electron beam or as a result of dissolving too much host phase into the melt during the homogenization procedure).

ity overall, melt compositions for a given rock-type show much smaller variation, and the relative differences in composition are what would be expected during fractional crystallization.

An electron-microprobe traverse across a melt inclusion in quartz from Red Mountain, showing SiO_2, Al_2O_3, CaO, FeO, K_2O, and Cl concentrations in the inclusion and host quartz, is shown in Figure 4. Copper and zinc concentrations in melt inclusions from Red Mountain, Tyrone, and from the basaltic andesite of White Island, are summarized in Figure 5. All melt inclusions in quartz from Red Mountain quartz latite and in quartz from the Tyrone quartz monzonite have concentrations of Cu and Zn that are below our estimated detection-limits (~15 ppm for Cu and ~20 ppm for Zn). The actual values obtained have no significance; these data are plotted simply to illustrate the point that Cu and Zn concentrations for the quartz-hosted melt inclusions are lower than those in the Red Mountain andesite and the White Island basaltic andesite. Note that the Cu concentrations in melt inclusions from the Meadow Valley andesite are about 20–40 times higher compared to melt inclusions in the Red Mountain quartz latite, consistent with whole-rock copper contents determined by Simons (1972).

The H_2O contents of melt inclusions were calculated from electron-microprobe results, assuming that differences from 100 wt% totals represent H_2O in the glass. We recognize that this is a somewhat simplistic assumption that ignores possible contributions from carbon (in carbon dioxide) and other light elements not included in the analytical scheme. Data are listed in Table 1 and shown on Figure 6. Anderson (1973, 1979) and Devine *et al.* (1995) have shown that the EPMA difference technique is valid for glasses containing more than about 1 wt% H_2O. The H_2O concentrations of melt inclusions in quartz determined by the EPMA difference technique vary significantly, from less than 2 wt% to greater than 8 wt%. Contents of H_2O in melt inclusions in pyroxene from the Red Mountain andesite and White Island basaltic andesite are less than 3 wt% (Fig. 6). In spite of the relatively large errors associated with EPMA determinations of H_2O content, it is clear that the H_2O contents of melt inclusions in quartz from syn- and post-mineralization intrusions are generally higher than H_2O contents of melt inclusions from pre-mineralization melt inclusions.

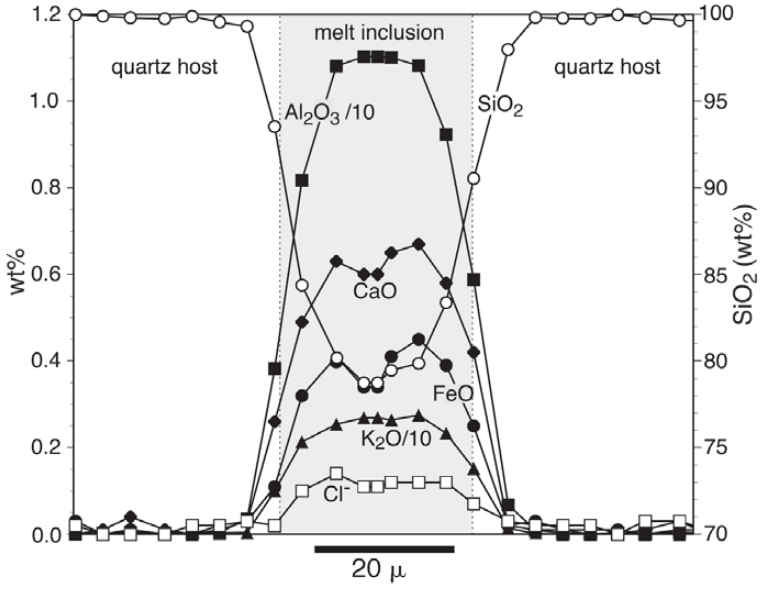

FIG. 4. Electron-microprobe traverse across a homogenized melt-inclusion in a quartz phenocryst from Red Mountain, Arizona. The electron beam size was 10 × 8 μm. The step size along the traverse is 4 μm. The CaO, FeO and Cl concentrations are plotted in weight percent, and Al_2O_3 and K_2O concentrations are in weight percent divided by 10. The SiO_2 concentration along the traverse is shown on the right axis. The shaded area represents compositions monitored partially or completely within the melt inclusion.

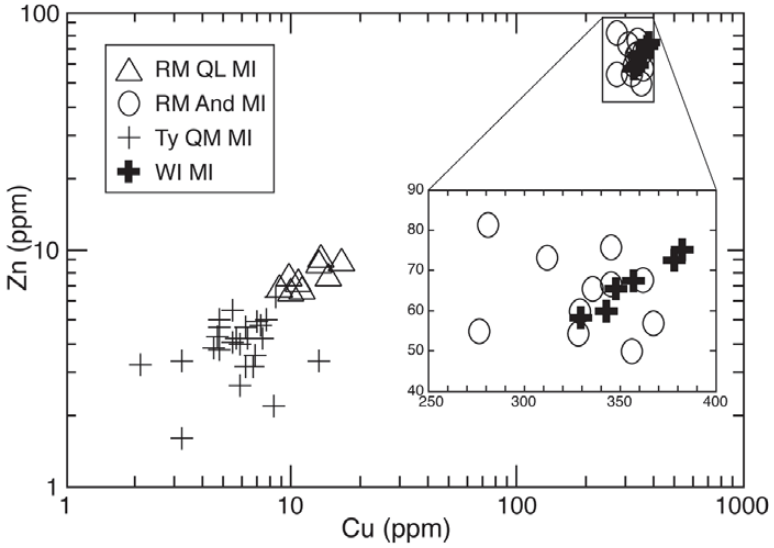

FIG. 5. Variation diagram for Cu and Zn concentrations of melt inclusions. Symbols are the same as in Figure 3, with the added bold cross symbol (WI MI) representing melt inclusions in plagioclase and pyroxene from White Island, New Zealand. The inset shows an enlargement of the area containing data for melt inclusions in Red Mountain Meadow Valley andesite and White Island basaltic andesite.

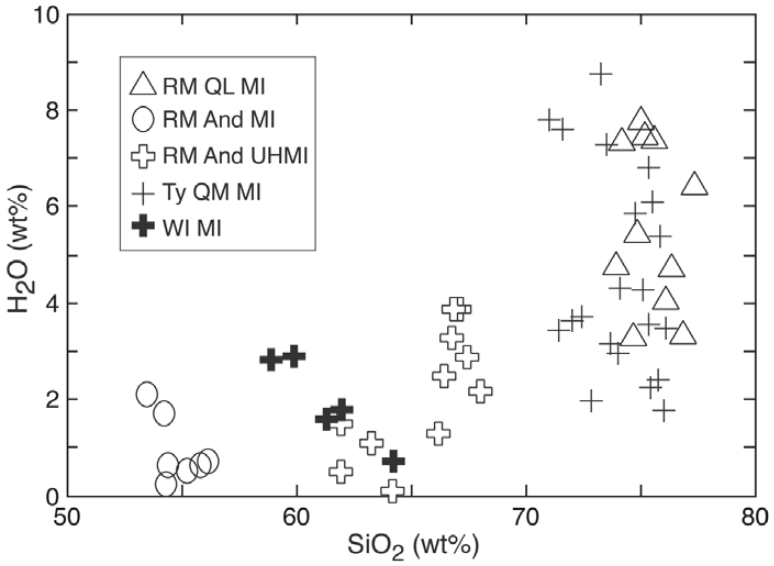

FIG. 6. H_2O content as function of SiO_2 concentration for melt inclusions. All inclusions contain only glass except for the Red Mountain unheated melt inclusions in andesite (RM And UHMI).

Discussion

Homogenization of crystallized melt-inclusions provides valuable information concerning the origin of melts, including the temperature of trapping as well as the state of the system. For example, was the melt volatile-saturated? Which phases were crystallizing at the time the melt was trapped? Moreover, homogenization is required before the volatile concentration of the melt can be determined. However, heating to homogenization is fraught with problems, not the least of which is decrepitation or re-equilibration of the inclusions. In the present study, decrepitation of all but the largest inclusions was minimized by heating the inclusions under confining pressure. The consistency of results from individual samples, as well as the expected differences between samples from different rock-types, suggests that re-equilibration during homogenization was minimal.

One unresolved concern relates to addition of components to the melt from the inclusion walls during the homogenization process. It is clear from observations of inclusions before and after homogenization that significant amounts of host material are dissolved into the melt (Fig. 1). During homogenization of melt inclusions in quartz (or any other host), either too much or too little host may be incorporated back into the melt. As an example, Webster & Duffield (1991) noted that failure to reheat glass- and crystal-bearing inclusions in quartz resulted in SiO_2 concentrations that were too low, because SiO_2 that crystallized onto the walls was not incorporated back into the melt. Results obtained here suggest that heating beyond the homogenization temperature may not significantly affect the SiO_2 concentration of the melt for inclusions hosted by quartz. As noted earlier, initial attempts to homogenize melt inclusions involved heating the inclusions at atmospheric pressure in the Linkam stage. Two inclusions (RM148B–1 and RM148B–2; Table 1) from the Red Mountain quartz latite homogenized at 915°C when heated in the Linkam stage. All other similar inclusions in the quartz latite homogenized between about 810° and 835°C when heated in a pressure vessel. In spite of the approximately 100°C difference in the temperature, the inclusions have essentially the same SiO_2 concentrations (Fig. 2, Table 1).

When plotted in the system Ab–Or–Qtz, normative compositions of quartz-hosted melt inclusions from Red Mountain and Tyrone define linear trends (Figs. 7A, B). Previous investigators (Frezzotti 1992, Varela 1994) also observed a linear trend in studies of melt inclusions from silicic igneous systems that underwent extensive subsolidus hydrothermal alteration. These investigators attributed the linear trend to interaction of the melt inclusions with circulating hydrothermal fluids. Quartz phenocrysts from Red Mountain and Tyrone show evidence of widespread hydrothermal activity in the form of abundant cross-cutting planes of aqueous inclusions. Many of these trails clearly have intersected melt inclusions. Such inclusions were avoided in this study, but it is likely that many melt inclusions that did not appear to be intersected by aqueous inclusions had nevertheless undergone some alteration.

The Red Mountain inclusions define a trend that projects from the interior of the ternary system toward the Qtz–Or join (Fig. 7A). This trend has been inter-

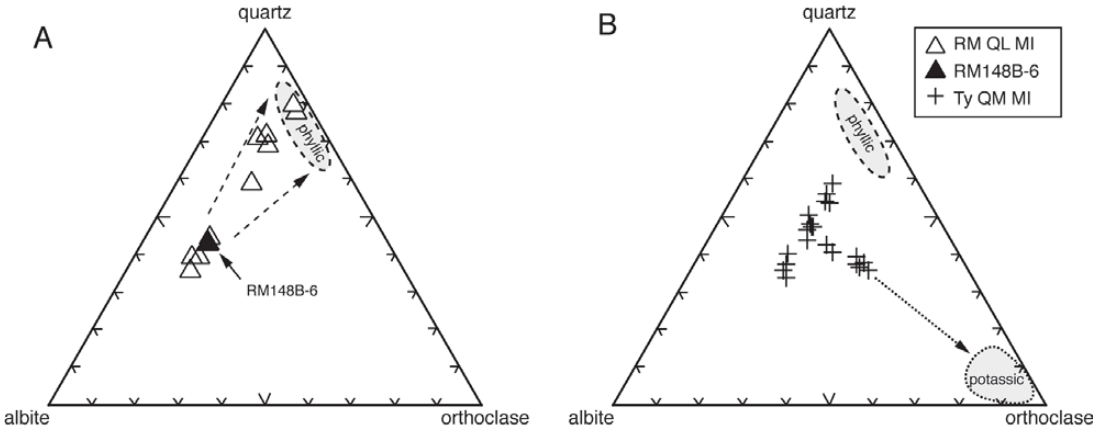

FIG. 7. Chemical evolution of melt inclusions as a result of interaction with hydrothermal fluids at Red Mountain, Arizona, (A) and Tyrone, New Mexico (B). The Red Mountain data are consistent with alteration of some melt inclusions by fluids with compositions near the quartz-rich end of the quartz–orthoclase join. This trend is considered to reflect interaction of the melt inclusion with fluids responsible for phyllic alteration. Compositions of melt inclusions at Tyrone define two trends, one that is similar to the Red Mountain phyllic trend, and one that projects to the orthoclase apex, and considered to reflect interaction with fluids responsible for potassic alteration.

preted to indicate that the melt inclusions were altered by the same fluids responsible for phyllic alteration in the deposit (Frezzotti 1992). Some melt inclusions from Tyrone show a similar trend, as well as a trend directly toward the Or apex (Fig. 7B). This latter trend is assumed to reflect alteration by fluids associated with potassic alteration, as has previously been recognized by Varela (1994).

The alteration trend shown of Figure 7A for Red Mountain starts at a composition of approximately $Qtz_{40}Or_{20}Ab_{40}$, and extends toward the quartz–orthoclase join. If the trend toward the Qtz–Or join is the result of alteration of the original melt, we can interpret the grouping of melt-inclusion compositions near $Qtz_{40}Or_{20}Ab_{40}$ to represent the original unaltered melt trapped in the quartz. To test this interpretation, the composition of the melt predicted by the crystallization model of Burnham (1997) was compared to the melt-inclusion compositions. For this analysis, melt inclusion RM148B–6, whose composition lies within the group of inclusions near $Qtz_{40}Or_{20}Ab_{40}$ (Fig. 7A, Table 1) was used. Model input includes the melt composition, the estimated H_2O content in the melt (or one can input an activity of H_2O equal to 1 to indicate an H_2O-saturated melt), and pressure. In our model, we used the melt composition obtained by EPMA analysis of RM148B–6 and an activity of H_2O equal to 1 (we did not correct the activity for the effect of dissolved salt or volatiles on H_2O activity). The model predicts the liquidus temperature for the melt, as well as the solubility of H_2O at the pressure that was selected. In our example, the input pressure was varied until the predicted H_2O content of the melt agreed with that inferred from EPMA analysis of the melt inclusion. The calculated pressure corresponding to the measured H_2O content (4.7 wt%) for melt inclusion RM148B–6 is 1.4 kbar. More importantly, the plagioclase plus quartz liquidus temperature predicted by the model is 810°C, identical to the measured temperature of homogenization. The calculated phase-behavior thus agrees with the observation that the plagioclase and the H_2O vapor bubble disappear simultaneously at the homogenization temperature of 810°C.

Contribution of Melt Inclusions to Understanding of Ore-Forming Processes

The goal of this study was not to conduct a detailed study of melt inclusions in porphyry copper deposits, but rather to develop a protocol for studying melt inclusions in this and similar types of deposit. However, the limited amount of data obtained here do serve to illustrate the significant potential of melt inclusions in studies of porphyry copper deposits. In particular, melt inclusions provide the best means, if not the only one, to determine the chemical composition of pristine early pre- and syn-mineralization magmas in these systems, including the metal budgets of these early magmas.

In the orthomagmatic model for the formation of porphyry copper deposits, the metals are derived from the magma that generated the host pluton (Burnham 1967, 1997, Nielsen 1968, Lowell & Guilbert 1970, Guilbert & Lowell 1974, Hedenquist & Lowenstern 1994). During crystallization, the hydrous, metal-bearing magma becomes saturated in H_2O and exsolves a saline hydrothermal fluid. Chlorine is partitioned into this magmatic aqueous fluid (Candela & Holland 1986, Cline & Bodnar 1991), and this promotes the extraction of copper and other metals from the magma as chloride complexes (Candela 1989). During the early crystallization of porphyry-related magmas, the metal concentration of the melt is generally assumed to increase as anhydrous, generally base-metal-free minerals crystallize (Candela & Piccoli 1995). Of course, metals can be depleted during this early stage of crystallization if minerals that incorporate base metals, including sulfides and perhaps some silicates such as biotite, also are forming. Once H_2O saturation is reached, experimental and theoretical studies agree that copper will be strongly partitioned into the exsolving aqueous phase, rapidly depleting the melt. According to this scenario, we should expect to find relatively metal-rich (or, at the very least, not significantly metal-depleted) melts early in the magmatic history of a porphyry copper system, and metal-poor melts after the magma has reached H_2O saturation.

In this scenario, the Meadow Valley andesite at Red Mountain and the basaltic andesite from White Island are interpreted to represent the pre-mineralization magmas in porphyry-copper systems. The Red Mountain system evolved through a copper mineralization stage (albeit, non-economic at the present time), whereas the White Island system is expected to reach the copper mineralization stage at some time during the next few tens to hundreds of thousands of years (Rapien *et al.* 2003). As noted previously, the quartz latite at Red Mountain is spatially and temporally associated with mineralization, and is considered to represent the causative intrusion, whereas the Stage-IV quartz monzonite from Tyrone was intruded after mineralization, although it is part of the same magmatic event that produced the mineralization. Melt inclusions in the studied samples thus represent magmas trapped before, during and following mineralization in porphyry copper systems.

Based on the lack of aqueous fluid inclusions in pyroxene and plagioclase phenocrysts, the andesite at Red Mountain did not reach saturation in H_2O. Conversely, quartz phenocrysts from the Red Mountain quartz latite contain abundant magmatic aqueous fluid inclusions (Bodnar 1991, 1995, Beane & Bodnar 1995, Roedder & Bodnar 1997), indicating that the magma was saturated in H_2O at the time the phenocrysts and their contained melt inclusions formed. Copper contents of melt inclusions in Red Mountain Meadow Valley andesite are significantly elevated compared to those in the quartz latite (Fig. 6). We interpret this difference to re-

flect the loss of copper from the melt to the exsolving magmatic aqueous phase to produce the ore-forming fluid. This interpretation is consistent with theoretical models of Cline & Bodnar (1991) for the Yerington system, and Burnham (1997) for the Bingham system. Moreover, it is consistent with the observation that magmatic halite-bearing inclusions in porphyry copper deposits contain ubiquitous chalcopyrite as a daughter mineral (Nash 1976, Roedder 1971, Bodnar 1995), and with the observation that magmatic fluids in silicic igneous systems have copper contents in the range 1000–10000 ppm (Bodnar 1999).

Results obtained here are consistent with results of laboratory, experimental and theoretical studies indicating that early magmas transport ore metals into the porphyry copper system. The metal concentrations continue to increase as the magma evolves, until the melt reaches H_2O saturation, at which point metals are quantitatively transferred from the melt into the magmatic aqueous phase. In many porphyry systems, metals may remain in solution for some unknown period of time until the solutions cool and mix with meteoric water and precipitate (Beane & Titley 1981). It is likely that some metals are deposited and remobilized numerous times as the system evolves. For example, analyses of fluid (Bodnar 1995) and melt inclusions indicate that Zn is an important component of the early magmatic-hydrothermal fluids, yet zinc mineralization in porphyry deposits is generally associated with the latest, peripheral, low-temperature mineralization event (Lowell & Guilbert 1970). Either zinc remains in solution until very late in the hydrothermal history of the system, or zinc is continuously deposited and subsequently remobilized as the hydrothermal system collapses. Studies of melt inclusions and associated magmatic hydrothermal inclusions offer the possibility to resolve this and similar questions concerning the source and transport and depositional mechanisms for metals in magmatic hydrothermal ore deposits.

Conclusions

Melt inclusions are common in porphyry copper deposits, but relatively few data are available on melt inclusions from these deposits. The paucity of studies is related to the fact that the melt inclusions are not easily recognized; most are partly to completely crystallized. Moreover, the high H_2O content of melts associated with ore formation results in decrepitation of most larger inclusions, either in nature following entrapment or during later laboratory studies to homogenize the inclusions. This problem is exacerbated by the numerous planes of aqueous inclusions that crosscut the host minerals. Some of these intersect the melt inclusions, altering their composition. Finally, studies of melt inclusions in porphyry copper deposits are limited because somewhat specialized equipment is required to homogenize the inclusions under high confining pressure to prevent (or minimize) leakage and decrepitation.

Preliminary data from melt inclusions from porphyry copper deposits show a consistent progression from silica-poor to silica-rich compositions during evolution of the ore-related magmas. Early pre-mineral melts are H_2O-undersaturated, whereas later syn- and post-mineral melts are H_2O saturated. Copper and zinc concentrations are high in melt inclusions considered to represent pre-mineral melts at both Red Mountain, Arizona, and White Island, New Zealand. Conversely, syn- and post-mineralization melts at Red Mountain, Arizona, and Tyrone, New Mexico, are depleted in copper and zinc compared to the earlier melts. The results are consistent with models that suggest that copper and zinc are extracted from the melt by high-salinity magmatic fluids, producing a metal-charged hydrothermal solution and leaving behind a metal-depleted melt.

Acknowledgements

The authors thank Todd Solberg for assistance with EPMA analysis of melt inclusions, and Csaba Szabo for guidance during the course of this work. Jim Quinlan (Kerr–McGee) and Ralph Stinson (Phelps Dodge) are thanked for providing access to samples and information related to the Red Mountain and Tyrone deposits, respectively. Wayne Burnham is thanked for kindly providing a copy of the unpublished Holloway and Burnham Fortran program used to calculate equilibrium conditions for melt inclusions. Jim Beard, Barbara Bekken and Bob Tracy provided valuable comments on an earlier version of this manuscript. Comments and suggestions by Dan Kontak, Robert Martin, Robert Linnen and Rainer Thomas helped to clarify and improve the content and presentation. Funding for this work was provided by NSF grants EAR–9527034 and EAR–0125918 to RJB.

References

Anderson, A.T., Jr. (1973): The before-eruption water content of some high-alumina magmas. *Bull. Volcanol.* **37**, 530-552.

_____ (1979): Water in some hypersthenic magmas. *J. Geol.* **87**, 509-531.

_____ (1991): Hourglass inclusions: theory and application to the Bishop rhyolitic tuff. *Am. Mineral.* **76**, 530-547.

Beane, R.E. & Bodnar, R.J. (1995): Hydrothermal fluids and hydrothermal alteration in porphyry copper deposits. *In* Porphyry Copper Deposits of the American Cordillera (F.W. Pierce & J.G. Bohm, eds.). *Arizona Geological Society Digest* **20**, 83-93.

_____ & Titley, S.R. (1981): Porphyry copper deposits. II. Hydrothermal alteration and mineralization. *Econ. Geol., 75th Anniv. Vol.*, 235-263.

BODNAR, R.J. (1991): Can we recognize magmatic fluid inclusions in fossil hydrothermal systems based on room temperature phase relations and microthermometric behavior? Japan–U.S. Seminar on Magmatic Contributions to Hydrothermal Systems (Kagoshima and Ebino, Japan), Extended Abstr., 17-20.

_____ (1995): Fluid inclusion evidence for a magmatic source for metals in porphyry copper deposits. *In* Magmas, Fluids and Ore Deposits (J.F.H. Thompson, ed.). *Mineral. Assoc. Can., Short-Course Vol*. **23**, 139-152.

_____ (1999): Hydrothermal solutions. *In* Encyclopedia of Geochemistry (C.P. Marshall & R.W. Fairbridge, eds.). Kluwer, Dordrecht, The Netherlands (333-337).

_____ (2003): Re-equilibration of fluid inclusions. *In* Fluid Inclusions: Analysis and Interpretation (I. Samson, A. Anderson, & D. Marshall, eds.). *Mineral. Assoc. Can., Short-Course Vol.* **32**, 213-230.

BURNHAM, C.W. (1967): Hydrothermal fluids at the magmatic stage. *In* Geochemistry of Hydrothermal Ore Deposits (H.L. Barnes, ed.). Holt, Rinehart, and Winston, New York, N.Y. (34-76).

_____ (1979): Magmas and hydrothermal fluids. *In* Geochemistry of Hydrothermal Ore Deposits (H.L. Barnes, ed.; 2nd edition). J. Wiley and Sons, New York, N.Y. (71-136).

_____ (1997): Magmas and hydrothermal fluids. *In* Geochemistry of Hydrothermal Ore Deposits (H.L. Barnes, ed.; 3rd edition). J. Wiley and Sons, New York, N.Y. (63-124).

CANDELA, P.A. (1989): Magmatic ore-forming fluids: thermodynamic and mass transfer calculations of metal concentrations. *In* Ore Deposition Associated with Magmas (J.A. Whitney & A.J. Naldrett, eds.). *Rev. Econ. Geol*. **4**, 223-233.

_____ & HOLLAND, H.D. (1986): A mass transfer model for copper and molybdenum in magmatic hydrothermal systems: origin of porphyry-type ore deposits. *Econ. Geol.* **81**, 1-19.

_____ & PICCOLI, P.M. (1995): Model ore-metal partitioning from melts into vapor and vapor–brine mixtures. *In Magmas, Fluids and Ore Deposits* (J.F.H. Thompson, ed.). *Mineral. Assoc. Can., Short-Course Vol.* **23**, 101-127.

CLINE, J.S. & BODNAR, R.J. (1991): Can economic porphyry copper mineralization be generated by a typical calc-alkaline melt? *J. Geophys. Res.* **96**, 8113-8126.

CLOCCHIATTI, R. (1975): Les inclusions vitreuses des cristaux de quartz. Étude optique, thermo-optique et chimique. Applications géologiques. *Soc. Géol. France, Mém*. **122**.

CORN, R.M. (1975): Alteration-mineralization zoning, Red Mountain, Arizona. *Econ. Geol.* **70**, 1437-1447.

COX, D.P. (1986): Descriptive model for porphyry Cu. *In* Mineral Deposit Models (D.P. Cox, & D.A. Singer, eds.). *U.S. Geol. Surv., Bull.* **1693** (p. 76).

DANYUSHEVSKY, L.V., DELLA-PASQUA, F.N. & SOKOLOV, S. (2000): Re-equilibration of melt inclusions trapped by magnesian olivine phenocrysts from subduction-related magmas: petrological implications. *Contrib. Mineral. Petrol.* **138**, 68-83.

_____, MCNEILL, A.W. & SOBOLEV, A.V. (2002): Experimental and petrological studies of melt inclusions in phenocrysts from mantle-derived magmas: an overview of techniques, advantages and complications. *Chem. Geol.* **183**, 5-24.

DAVIDSON, P. & KAMENETSKY, V.S. (2001): Immiscible and continuous felsic melt–fluid evolution within the Rio Blanco porphyry system, Chile: evidence from fluid inclusions in magmatic quartz. *Econ. Geol.* **96**, 1921-1929.

DEVINE, J.D., GARDNER, J.E., BRACK, H.P., LAYNE, D.E. & RUTHERFORD, M.J. (1995): Comparison of microanalytical methods for estimating H_2O contents of silicic volcanic glasses. *Am. Mineral.* **80**, 319-329.

DUHAMEL, J.E., COOK, S.S. & KOLESSAR, J. (1995): Geology of the Tyrone porphyry copper deposit, New Mexico. *In* Porphyry Copper Deposits of the American Cordillera (F.W. Pierce & J.G. Bohm, eds.). *Arizona Geological Society Digest* **20**, 464-472.

FEDELE, L., BODNAR, R.J., DEVIVO, B. & TRACY, R. (2003): Melt inclusion geochemistry and computer modeling of trachyte petrogenesis at Ponza, Italy. *Chem. Geol*. **194**, 81-104.

FIALIN, M., RÉMY, H., RICHARD, C. & WAGNER, C. (1999): Trace element analysis with the electron microprobe: new data and perspectives. *Am. Mineral*. **84**, 70-77

FREZZOTTI, M.L. (1992): Magmatic immiscibility and fluid phase evolution in the Mount Genis granite (southeastern Sardinia, Italy). *Geochim. Cosmochim. Acta* **56**, 21-33.

_____ (2001): Silicate-melt inclusions in magmatic rocks: applications to petrology. *Lithos* **55**, 273-299.

GUILBERT, J. M. & LOWELL, J.D. (1974): Variations in zoning patterns in porphyry ore deposits. *Can. Inst. Mining Metall., Bull.* **67**, 99-109.

_____ & PARKS, C.F., JR. (1986): *The Geology Of Ore Deposits*. W.H. Freeman and Co., New York, N.Y.

HALTER, W.E., PETTKE, T., HEINRICH, C.A. & ROTHEN-RUTISHAUSER, B. (2002): Major to trace element analysis of melt inclusions by laser-ablation ICP–MS; methods of quantification. *Chem. Geol*. **183**, 63-86.

HEDENQUIST, J.W. & LOWENSTERN, J.B. (1994): The role of magmas in the formation of hydrothermal ore deposits. *Nature* **370**, 519-526.

LOWELL, J.D. & GUILBERT, J.M. (1970): Lateral and vertical zonation in porphyry ore deposits. *Econ. Geol*. **65**, 373-408.

LOWENSTERN, J.B. (1994): Dissolved volatile contents in an ore-forming magma. *Geology* **22**, 893-896.

_____ (1995): Application of silicate-melt inclusions to the study of magmatic volatiles. *In* Magmas, Fluids and Ore Deposition (J.F.H. Thompson, ed.). *Mineral. Assoc. Can., Short-Course Vol.* **23**, 71-98.

LYNTON, S.J., CANDELA, P.A. & PICCOLI, P.M. (1993): An experimental study of the partitioning of copper between pyrrhotite and a high silica rhyolite melt. *Econ. Geol*. **88**, 901-915.

NANEY, M.T. (1984): A grinding/polishing tool to aid thin section preparation of small samples. *Am. Mineral.* **69**, 404-405.

NASH, T.J. (1976): Fluid-inclusion petrology – data from porphyry copper deposits and applications to exploration. *U.S. Geol. Surv., Prof. Pap.* **907–D**.

NIELSEN, R.L. (1968): Hypogene texture and mineral zoning in a copper-bearing granodiorite stock, Santa Rita, New Mexico. *Econ. Geol*. **63**, 37-50.

_____, MICHAEL, P.J. & SOURS-PAGE, R. (1998): Chemical and physical indicators of compromised melt inclusions. *Geochim. Cosmochim Acta* **62**, 831-838.

POUCHOU, J.L. & PICHOIR, F. (1985): "PAP" procedure for improve quantitative microanalysis. *Microbeam Analysis* **20**, 104-105.

QIN, Z., LU, F. & ANDERSON, A.T., JR. (1992): Diffusive reequilibration of melt and fluid inclusions. *Am. Mineral*. **77**, 565-576.

RAPIEN, M.H. (1998): *Geochemical Evolution at White Island, New Zealand*. M.S. thesis, Virginia Tech, Blacksburg, Virginia.

_____, BODNAR, R.J., SIMMONS, S., SZABÓ, C.S., WOOD, C.P. & SUTTON, S.R. (2003): Melt inclusion study of the embryonic porphyry copper system at White Island, New Zealand. *Soc. Econ. Geol., Spec. Publ.* **10**, 41-59.

ROEDDER, E. (1971): Fluid inclusion studies on the porphyry-type ore deposits at Bingham, Utah, Butte, Montana, and Climax, Colorado. *Econ. Geol.* **66**, 98-120.

_____ (1979): Origin and significance of magmatic inclusions. *Bull. Minéral*. **102**, 487-510.

_____ (1984): Fluid Inclusions. *Rev. Mineral*. **12**.

_____ & BODNAR, R.J. (1997): Fluid inclusion studies of hydrothermal ore deposits. *In* Geochemistry of Hydrothermal Ore Deposits (H.L. Barnes, ed.; 3rd edition). John Wiley & Sons, New York, N.Y. (657-698).

SCHMIDT, C., CHOU, I-MING, BODNAR, R.J. & BASSETT, W.A. (1998): Microthermometric analysis of synthetic fluid inclusions in the hydrothermal diamond-anvil cell. *Am. Mineral*. **83**, 995-1007.

SIMONS, F.S. (1972): Mesozoic stratigraphy of the Patagonia Mountains and adjoining areas, Santa Cruz County, Arizona. *U.S. Geol. Surv., Prof. Pap.* **658–E**.

SKIRIUS, C.M., PETERSON, J.W & ANDERSON, A.T., JR. (1990): Homogenizing rhyolitic glass inclusions from the Bishop Tuff. *Am. Mineral*. **75**, 1381-1398.

SOBOLEV, A.V. (1996): Melt inclusions in minerals as a source of principal petrologic information. *Petrology* **4**, 228-239.

_____, DMITRIEV, L.V., BARSUKOV, V.L., NEVSOROV, V.N. & SLUTSKY, A.B. (1980): The formation conditions of high magnesium olivines from the mono-mineral fraction of Luna-24 regolith. Proc. 11th Lunar and Planet. Sci. Conf., 105-116.

STERNER, S.M. & BODNAR, R.J. (1989): Synthetic fluid inclusions. VII. Reequilibration of fluid inclusions in quartz during laboratory-simulated metamorphic uplift. *J. Metamorph. Geol*. **7**, 243-260.

STUDENT, J.J. (2002): *Silicate Melt Inclusions in Igneous Petrogenesis.* Ph.D. dissertation, Virginia Tech, Blacksburg, VA. Available online at: http://scholar.lib.vt.edu/theses/available/etd–08192002–150340/

_____ & BODNAR, R.J. (1996): Melt inclusion microthermometry: petrologic constraints from the H_2O-saturated haplogranite system. *Petrology* **4**, 291-306.

_____ & _____ (1999): Synthetic fluid inclusions. XIV. Microthermometric and compositional analysis of coexisting silicate melt and aqueous fluid inclusions trapped in the haplogranite–H_2O–NaCl–KCl system at 800°C and 2000 bars. *J. Petrol.* **40**, 1509-1525.

THOMAS, J.B., BODNAR, R.J., SHIMIZU, N. & SINHA, A.K. (2002): Determination of zircon/melt trace element partition coefficients from SIMS analysis of melt inclusions in zircon. *Geochim. Cosmochim. Acta* **66**, 2887-2902.

THOMAS, R. (1994a): Estimation of viscosity and water content of silicate melts from melt inclusion data. *Eur. J. Mineral.* **6**, 511-535.

_____ (1994b): Fluid evolution in relation to the emplacement of the Variscan granites in the Erzgebirge region: a review of the melt and fluid inclusion evidence. *In* Metallogeny of Collisional Orogens Focussed on the Erzgebirge and Comparable Metallogenetic Settings (R. Seltmann, H. Kämpf & P. Möller, eds.). Czech Geol. Survey, Prague, Czech Republic (70-81).

VARELA, M.E. (1994): Silicate-melt and fluid inclusions in rhyolitic dykes, Los Manantiales mining district, Argentina. *Eur. J. Mineral.* **6**, 837-854.

VITYK, M.O. & BODNAR, R.J. (1995): Textural evolution of synthetic fluid inclusions in quartz during re-equilibration, with applications to tectonic reconstruction. *Contrib. Mineral. Petrol.* **121**, 309-323.

_____, _____ & DUDOK, I. (1995): Natural and synthetic re-equilibration textures of fluid inclusions in quartz (Marmarosh Diamonds): evidence for refilling under conditions of compressive loading. *Eur. J. Mineral.* **7**, 1071-1087.

WEBSTER, J.D. & DUFFIELD, W.A. (1991): Volatiles and lithophile elements in Taylor Creek rhyolite: constraints from glass inclusion analysis. *Am. Mineral*. **76**, 1628-1645.

_____, THOMAS, R., RHEDE, D., FÖRSTER, H.-J. & SELTMANN, R. (1997): Melt inclusions in quartz from an evolved peraluminous pegmatite: geochemical evidence for strong tin enrichment in fluorine-rich and phosphorus-rich residual liquids. *Geochim. Cosmochim. Acta* **61**, 2589-2604.

WILLIAMS, T.J., CANDELA, P.A. & PICCOLI, P.M. (1995): The partitioning of copper between silicate melts and two-phase aqueous fluids: an experimental investigation at 1 kbar, 800°C and 0.5 kbar, 850°C. *Contrib. Mineral. Petrol.* **121**, 388-399.

YANG, K. & BODNAR, R.J. (1994): Magmatic-hydrothermal evolution in the "bottoms" of porphyry copper systems: evidence from silicate melt and aqueous fluid inclusions in granitoid intrusions in the Gyeongsang Basin, South Korea. *Int. Geol. Rev*. **36**, 608-628.

Received January 3, 2004, revised manuscript accepted October 18, 2004.

We acknowledge the financial support of the Government of Canada, through the Publications Assistance Program (PAP), toward our mailing costs.

PUBLICATIONS MAIL AGREEMENT NO. 40011842 • REGISTRATION NO. 09397
RETURN UNDELIVERABLES CANADIAN ADDRESSES TO CIRCULATION DEPT.
330-123 MAIN STREET, TORONTO ON M5W 1A1

Email: **circdept@publisher.com**